Higgs modes in proximized superconducting systems

V. L. Vadimov,[1,2,*] I. M. Khaymovich,[3] and A. S. Mel'nikov[1,2]

[1]*Institute for Physics of Microstructures, Russian Academy of Sciences, 603950 Nizhny Novgorod, GSP-105, Russia*

[2]*Physics of Nanostructures and Nanoelectronics, University of Nizhny Novgorod, 23 Gagarin Avenue, 603950 Nizhny Novgorod, Russia*

[3]*Max Planck Institute for the Physics of Complex Systems, Nöthnitzer Straße 38, 01187 Dresden, Germany*

(Received 6 June 2019; revised manuscript received 10 August 2019; published 16 September 2019)

The proximity effect in hybrid superconducting–normal-metal structures is shown to affect strongly the coherent oscillations of the superconducting order parameter Δ known as the Higgs modes. The standard Higgs mode at frequency 2Δ is damped exponentially by the quasiparticle leakage from the primary superconductor. Two new Higgs modes with the frequencies depending on both the primary and induced gaps in the hybrid structure are shown to appear due to the coherent electron transfer between the superconductor and the normal metal. Altogether, these three modes determine the long-time asymptotic behavior of the superconducting order parameter disturbed either by the electromagnetic pulse or the quench of the system parameters and thus are of crucial importance for the dynamical properties and restrictions on the operating frequencies for superconducting devices based on the proximity effect used, e.g., in quantum computing, in particular, with topological low-energy excitations.

DOI: 10.1103/PhysRevB.100.104515

I. INTRODUCTION

The progress of modern nanotechnology opens new horizons for engineering superconducting correlations in various hybrid structures and creating, in fact, novel types of artificial superconducting materials with controllable properties [1–11]. The proximity phenomenon arising in a nonsuperconducting material from the electron exchange with a primary superconductor can generate the induced superconducting ordering in a wide class of materials, including unconventional ones [1–5,8–11]. The resulting superconducting state in these materials can controllably reveal the exotic properties very rarely found in natural metals or alloys and strongly different from the ones of the primary superconductor. The induced Cooper pairs can change, e.g., their spin structure from the singlet to a triplet one in the presence of strong spin-orbit coupling and Zeeman (or exchange) field [1,9,10]. This spin transformation affects, of course, the momentum space structure of pairs: the routine *s*-wave condensate can turn into an exotic *p*-wave one. The resulting Cooper pair structure leads to the formation of topological low-energy excitations such as Majorana fermions [1,9–11] and possesses a high potential for the development of new types of nanoelectronic devices perspective for applications in quantum computing, quantum information processing, quantum annealing, quantum memory, and more [9,10].

It is no wonder that the study of both equilibrium and nonequilibrium spectral and transport properties of these systems with an engineered superconducting state has recently become one of the central research directions in condensed-matter physics. While dc properties of these structures have been investigated in numerous theoretical and experimental works, the dynamic effects and, in particular, high-frequency response remain an appealing problem which definitely deserves deeper understanding. Indeed, the limitations on the operating frequencies for the above-mentioned proximized devices [12–17] can be solely given by the dynamic characteristics of their induced superconducting ordering. The nonlinear dynamic effects are also known to provide a new route to the fascinating physics of coherent modification of the density of states, etc., induced by microwave irradiation [18,19].

Clearly, as typical quantum computing devices operate at temperatures *well below* the gap of the primary superconductor, the study of the relaxation dynamics of the order parameter *close* to the critical temperature of the superconducting transition is irrelevant for their description. A more adequate theory can be obtained by considering the so-called coherent quantum-mechanical dynamics of the system, which neglects inelastic scattering processes. In addition, in superconducting systems with the unconventional pairing the dynamic response is known to provide important information about the order parameter structure [20,21] working as a spectroscopic tool [22]. The analogous method can provide insight into the internal structure of the primary and induced Cooper pairings in superconducting hybrids.

Indeed, even the linear dynamic response of the superconductor near equilibrium provides a detection method for the superconducting gap structure via the coherent order parameter oscillations known also as Higgs modes [23–28]. The name is given due to the analogy to the Higgs boson in particle physics [28]. In the low-temperature limit these near-equilibrium Higgs oscillations of the order parameter magnitude are described by the asymptotic long-time expression

*Present address: Department of Applied Physics, Aalto University, FI-00076 Aalto, Finland.

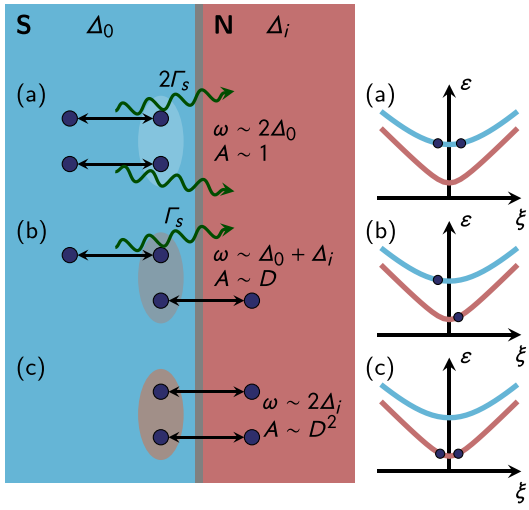

FIG. 1. Illustration of three Higgs modes in SIN structure, being coherent Cooper pair splitting-recovery processes with three different frequencies ω, decay rates, and amplitudes A.

$\Delta - \Delta_0 \sim \cos(2\Delta_0 t)/\sqrt{\Delta_0 t}$, where Δ_0 is the superconducting gap in equilibrium [23–27,29]. The Higgs mode was first detected using Raman spectroscopy in the superconductors with charge density wave ordering [30,31] as a peak at the frequency $2\Delta_0$ in the Raman spectrum of $2H$-$NbSe_2$ below the superconducting transition temperature. Recent progress with the terahertz (THz) experimental techniques allowed the direct observation of the order parameter oscillations using the pump-probe method [32]. The broadband pump excites a power-law relaxing Higgs mode at the frequency $2\Delta_0$, while the narrow-band pump with a well-defined frequency ω induces oscillations of the order parameter at the frequency 2ω. The resonant third-harmonic generation [33,34] provides evidence of the Higgs mode excitation in the superconductors. An alternative method of the Higgs mode detection through second-harmonic measurements was recently discovered for the current carrying states [35].

In this paper we address an important effect of the quasiparticle spectrum of the superconducting system on long-time dynamic properties of Higgs modes and apply it to a system with a proximity-induced superconducting gap. Key physical phenomena related to the presence of the induced gap are demonstrated in the example of a junction of the superconductor (S) and normal metal (N) coupled via an insulating barrier (I) with finite transparency. We analyze the distinctive features of the Higgs modes in this structure and make predictions for the experimentally accessible relevant quantities.

Let's first consider the qualitative picture of the Higgs dynamics in the SIN system (Fig. 1) before proceeding with further microscopic calculations. The Higgs modes in superconductors can be interpreted as a coherent splitting-recovery process of Cooper pairs. The energy difference between the ground state without quasiparticles and the excited state with two quasiparticles governs the frequency $2\Delta_0$ of this coherent superposition of the above states as each unpaired quasiparticle brings an additional energy Δ_0. Due to this simple qualitative reasoning we may expect the frequencies of the Higgs modes to be determined by the quasiparticle spectrum of the system. In the SIN structure the superconducting correlations penetrate to the normal metal and induce the hard gap Δ_i in the whole system, which is determined by the tunneling rate Γ_n from the normal metal to the superconductor, provided $\Gamma_n \ll \Delta_0$ [36]. The tunneling rate Γ_n can be interpreted as the inverse lifetime of the electron in the normal metal. It depends on the transparency of the barrier, the thickness of the normal subsystem, and the normal density of states at the Fermi level in the superconducting material.

We claim that in the SIN structure there are three Higgs modes corresponding to three possible processes shown in Fig. 1. First, as in the isolated superconductor, the Cooper pair may coherently split into two electrons, both located in the superconductor [Fig. 1(a)]. The energy $2\Delta_0$ of these unpaired electrons determines the frequency of this process. However, in the presence of the normal metal the Cooper pair splitting can be accompanied by the coherent tunneling process of either or both electrons [see Figs. 1(b) and 1(c), respectively]. The minimal energy of each electron which tunnels to the normal metal should be Δ_i, so the frequency of the corresponding Higgs mode is given by $\Delta_0 + \Delta_i$ and $2\Delta_i$ for $n_e = 1$ and 2 electrons tunneling to the normal metal, respectively. The amplitudes A of these modes are expected to be reduced by a factor of D^{n_e}, where D is the transparency of the barrier (provided $D \ll 1$). On top of that in the first two processes [Figs. 1(a) and 1(b)], the coherent superposition can be destroyed by the incoherent decay of each electron located in the superconductor to the normal metal (see green wavy lines in Fig. 1) because the hard gap in the spectrum of the whole system Δ_i is below the energy of the quasiparticle in the superconductor Δ_0. This effect results in an exponential damping of the Higgs modes with a rate Γ_s to each Δ_0 frequency contribution. The value Γ_s is the inverse lifetime of the electron in the superconductor determined by the tunneling rate from the superconductor to the normal metal. The inverse process of quasiparticle tunneling from the normal metal to the superconductor is suppressed because there are no quasiparticle states in the superconductor with energy of about Δ_i; thus, the relaxation rate of the Higgs modes does not depend on Γ_n, at least up to second order in the barrier transparency D^2. To sum up, the main result of our work can be written from the qualitative perspective as the following structure of the gap oscillations in a SIN system in the limit $\Gamma_s, \Gamma_n \ll \Delta_0$:

$$\delta\Delta \sim \frac{\cos(2\Delta_0 t)}{\sqrt{\Delta_0 t}} e^{-2\Gamma_s t} + D\frac{\cos[(\Delta_0+\Delta_i)t]}{(\Delta_0 t)^p} e^{-\Gamma_s t} + D^2\frac{\cos(2\Delta_i t)}{(\Delta_0 t)^q}, \tag{1}$$

with certain power-law decay rates p and q.

In Sec. II we introduce the microscopic model and the basic equations for the Green's functions. In Sec. III the self-consistent equations for the dynamics of the superconducting order parameter are derived. Section IV is devoted to the dynamics of the superconducting order parameter studied in the limit $\Delta_i = 0$. In Sec. V the possibility of the experimental observation of the Higgs modes in SIN systems is discussed. In Sec. VI we sum up the results.

II. MICROSCOPIC MODEL: BASIC EQUATIONS

This qualitative picture can be confirmed by the direct microscopic calculations. The considered SIN system can be described by the following tunneling Hamiltonian:

$$\hat{H} = \sum_{k\sigma} \xi_k^s \hat{a}_{k\sigma}^\dagger \hat{a}_{k\sigma} + \sum_k (\Delta \hat{a}_{k\uparrow}^\dagger \hat{a}_{\bar{k}\downarrow}^\dagger + \Delta^* \hat{a}_{\bar{k}\downarrow} \hat{a}_{k\uparrow}) + \sum_{l\sigma} \xi_l^n \hat{b}_{l\sigma}^\dagger \hat{b}_{l\sigma} + \sum_{kl\sigma} (\gamma_{kl} \hat{a}_{k\sigma}^\dagger \hat{b}_{l\sigma} + \gamma_{kl}^* \hat{b}_{l\sigma}^\dagger \hat{a}_{k\sigma}), \quad (2)$$

where $\hat{a}_{k\sigma}$ and $\hat{a}_{k\sigma}^\dagger$ are the electron annihilation and creation operators in the superconducting layer, k is the index of the single-electron state, σ is the projection of the electron spin, and $\bar{k}$ denotes the index of the state obtained from state k by the time inversion operation. The operators $\hat{b}_{l\sigma}$ and $\hat{b}_{l\sigma}^\dagger$ are the electron annihilation and creation operators in the normal layer. The last term describes the tunneling between the superconductor and the normal metal. Assuming the insulating layer to be dirty so that the electron momentum is not conserved, we consider the tunneling matrix elements γ_{kl} to be Gaussian uncorrelated random values $\langle \gamma_{kl} \gamma_{k'l'}^* \rangle = \gamma^2 \delta_{kk'} \delta_{ll'}$ [36,37]. This model approximately describes the tunneling junction if the magnitude of the tunneling matrix element γ^2 is equal to $\tau^2 S/(V_s V_n)$, where τ is the geometry-independent tunneling amplitude, S is the junction area, and V_s and V_n are the volumes of the superconducting and normal subsystems, respectively. The superconducting order parameter Δ is given by the self-consistency equation:

$$\Delta = \frac{\lambda}{V_s} \sum_k \langle \hat{a}_{k\uparrow} \hat{a}_{\bar{k}\downarrow} \rangle, \quad (3)$$

where λ is the pairing constant, V_s is the volume of the superconductor, and the brackets $\langle \cdots \rangle$ denote a quantum-mechanical averaging. Here we assume the thickness of the superconducting subsystem is small compared to the superconducting coherence length, so we can consider Δ to be homogeneous within the sample.

We study the dynamics of the system using the nonequilibrium Keldysh technique. Following the approach developed in [6,7,36,38,39], we introduce the Green's functions of the superconductor $\check{G}_{kk'}^{ss}(t,t')$, normal metal $\check{G}_{ll'}^{nn}(t,t')$, and two tunneling Green's functions, $\check{G}_{kl}^{sn}(t,t')$ and $\check{G}_{lk}^{ns}(t,t')$. These Green's functions are the 4×4 matrices in the Keldysh-Nambu space:

$$\check{G}_{kk'}^{\alpha\beta}(t,t') = \begin{pmatrix} \check{G}_{kk'}^{\alpha\beta(R)}(t,t') & \check{G}_{kk'}^{\alpha\beta(K)}(t,t') \\ 0 & \check{G}_{kk'}^{\alpha\beta(A)}(t,t') \end{pmatrix}, \quad (4)$$

where $\check{G}_{kk'}^{\alpha\beta(R/A/K)}$ are the retarded, advanced, and Keldysh Green's functions, respectively, and the indices α and β denote s and n. The equations for the Green's functions read

$$\begin{aligned} i\frac{\partial}{\partial t}\check{G}_{kk'}^{ss} - \check{H}_k^s \check{G}_{kk'}^{ss} - \sum_l \gamma_{kl} \check{\tau}_3 \check{G}_{lk'}^{ns} &= \delta(t-t')\delta_{kk'}, \\ i\frac{\partial}{\partial t}\check{G}_{lk}^{ns} - \check{H}_l^n \check{G}_{lk}^{ns} - \sum_{k'} \gamma_{k'l}^* \check{\tau}_3 \check{G}_{k'k}^{ss} &= 0, \\ i\frac{\partial}{\partial t}\check{G}_{ll'}^{nn} - \check{H}_n^s \check{G}_{ll'}^{nn} - \sum_k \gamma_{kl}^* \check{\tau}_3 \check{G}_{kl'}^{sn} &= \delta(t-t')\delta_{ll'}, \\ i\frac{\partial}{\partial t}\check{G}_{kl}^{sn} - \check{H}_k^s \check{G}_{kl}^{sn} - \sum_{l'} \gamma_{kl'} \check{\tau}_3 \check{G}_{l'l}^{nn} &= 0, \end{aligned} \quad (5)$$

$$\begin{aligned} i\frac{\partial}{\partial t}\check{G}_{ll'}^{nn} - \check{H}_n^s \check{G}_{ll'}^{nn} - \sum_k \gamma_{kl}^* \check{\tau}_3 \check{G}_{kl'}^{sn} &= \delta(t-t')\delta_{ll'}, \\ i\frac{\partial}{\partial t}\check{G}_{kl}^{sn} - \check{H}_k^s \check{G}_{kl}^{sn} - \sum_{l'} \gamma_{kl'} \check{\tau}_3 \check{G}_{l'l}^{nn} &= 0, \end{aligned} \quad (6)$$

where

$$\check{H}_k^s = \begin{pmatrix} \check{H}_k^s & 0 \\ 0 & \check{H}_k^s \end{pmatrix}, \quad \check{H}_k^s = \begin{pmatrix} \xi_k^s & \Delta \\ \Delta^* & -\xi_k^s \end{pmatrix}, \quad (7)$$

$$\check{H}_l^n = \begin{pmatrix} \check{H}_l^n & 0 \\ 0 & \check{H}_l^n \end{pmatrix}, \quad \check{H}_l^n = \begin{pmatrix} \xi_l^n & 0 \\ 0 & -\xi_l^n \end{pmatrix}, \quad (8)$$

$$\check{\tau}_3 = \begin{pmatrix} \check{\tau}_3 & 0 \\ 0 & \check{\tau}_3 \end{pmatrix}, \quad \check{\tau}_3 = \begin{pmatrix} 1 & 0 \\ 0 & -1 \end{pmatrix}. \quad (9)$$

The self-consistency condition takes the form

$$\Delta(t) = \frac{i\lambda}{4V} \sum_k \mathrm{Tr}\left[(\check{\tau}_1 + i\check{\tau}_2)\check{G}_{kk}^{ss(K)}(t,t)\right], \quad (10)$$

where 2×2 Pauli matrices are

$$\check{\tau}_1 = \begin{pmatrix} 0 & 1 \\ 1 & 0 \end{pmatrix}, \quad \check{\tau}_2 = \begin{pmatrix} 0 & -i \\ i & 0 \end{pmatrix}. \quad (11)$$

Using the Green's functions of the isolated superconductor and the normal metal, $\check{\mathcal{G}}_k^s$ and $\check{\mathcal{G}}_l^n$, we eliminate the tunneling Green's functions:

$$\begin{aligned} \check{G}_{lk}^{ns} &= \sum_{k'} \gamma_{k'l}^* \check{\mathcal{G}}_l^n \check{\tau}_3 * \check{G}_{k'k}^{ss}, \\ \check{G}_{kl}^{sn} &= \sum_{l'} \gamma_{kl'} \check{\mathcal{G}}_k^s \check{\tau}_3 * \check{G}_{l'l}^{nn}, \end{aligned} \quad (12)$$

where the asterisk $(*)$ denotes the convolution operation

$$(X * Y)(t,t') = \int X(t,t'') Y(t'',t')\, dt'' \quad (13)$$

and the Green's functions $\check{\mathcal{G}}_k^s$ and $\check{\mathcal{G}}_l^n$ satisfy the following equations:

$$\begin{aligned} i\frac{\partial}{\partial t}\check{\mathcal{G}}_k^s - \check{H}_k^s \check{\mathcal{G}}_k^s &= \delta(t-t'), \\ i\frac{\partial}{\partial t}\check{\mathcal{G}}_l^n - \check{H}_l^n \check{\mathcal{G}}_l^n &= \delta(t-t'). \end{aligned} \quad (14)$$

Thus, we can write two formally independent equations for the Green's functions in the superconductor and the normal metal:

$$i\frac{\partial}{\partial t}\check{G}_{kk'}^{ss} - \check{H}_k^s \check{G}_{kk'}^{ss} - \sum_{k''} \check{\Sigma}_{kk''}^s * \check{G}_{k''k'}^{ss} = \delta(t-t')\delta_{kk'}, \quad (15)$$

$$i\frac{\partial}{\partial t}\check{G}_{ll'}^{nn} - \check{H}_l^n \check{G}_{ll'}^{nn} - \sum_{l''} \check{\Sigma}_{ll''}^n * \check{G}_{l''l'}^{nn} = \delta(t-t')\delta_{ll'}, \quad (16)$$

where the self-energies of the superconductor and the normal metal are

$$\check{\Sigma}_{kk''}^s = \sum_l \gamma_{kl} \gamma_{k''l}^* \check{\tau}_3 \check{\mathcal{G}}_l^n \check{\tau}_3, \quad (17)$$

$$\check{\Sigma}_{ll''}^n = \sum_k \gamma_{kl}^* \gamma_{kl''} \check{\tau}_3 \check{\mathcal{G}}_k^s \check{\tau}_3. \quad (18)$$

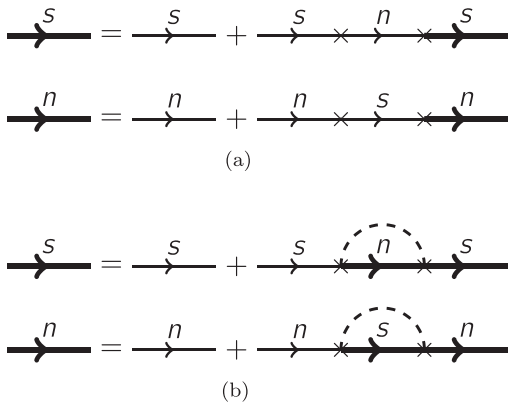

FIG. 2. Diagrams for the Green's functions in the superconductor and the normal metal. (a) Exact Dyson equation for the Green's functions (before averaging). (b) Self-consistent Born approximation for the averaged Green's function. The × symbol denotes tunneling; the dashed line denotes the correlator between the matrix elements of the tunneling operator.

These equations written in diagram form are shown in Fig. 2(a). These equations are not practical to use as they contain the tunneling matrix elements γ_{kl}, which are random quantities. One can average the equations over the random matrix elements, and the average of the product of the matrix elements can be expanded as sums of correlators due to the Wick theorem; thus, the averaged Green's function can be written as a sum of diagrams. We omit the diagrams with the intersecting correlators; thus, we neglect the vertex corrections. Such an approach is known as a self-consistent Born approximation. The diagrammatic form of the Dyson equation for this approximation is shown in Fig. 2(b). After averaging, the self-energies and the Green's function appear to be diagonal in the normal-mode picture and obey the following equations:

$$\begin{aligned} i\frac{\partial \check{G}_k^s}{\partial t} - \check{H}_k^s \check{G}_k^s - \check{\Sigma}^s * \check{G}_k^s &= \delta(t-t'), \\ i\frac{\partial \check{G}_l^n}{\partial t} - \check{H}_l^n \check{G}_l^n - \check{\Sigma}^n * \check{G}_l^n &= \delta(t-t'), \end{aligned} \tag{19}$$

$$\begin{aligned} \check{\Sigma}^s &= \gamma^2 \sum_l \check{\tau}_3 \check{G}_l^n \check{\tau}_3, \\ \check{\Sigma}^n &= \gamma^2 \sum_k \check{\tau}_3 \check{G}_k^s \check{\tau}_3. \end{aligned} \tag{20}$$

In the wide-band approximation the sum over the normal modes can be replaced by the integral over the normal energy $\sum_k \to \nu_s V_s \int d\xi_k^s$ ($\sum_l \to \nu_n V_n \int d\xi_l^n$):

$$\begin{aligned} \check{\Sigma}^s &= \frac{\Gamma_s}{\pi} \int \check{\tau}_3 \check{G}_l^n \check{\tau}_3 \, d\xi_l^n, \\ \check{\Sigma}^n &= \frac{\Gamma_n}{\pi} \int \check{\tau}_3 \check{G}_k^s \check{\tau}_3 \, d\xi_k^s, \end{aligned} \tag{21}$$

where we have introduced the tunneling rates of electrons from the superconductor $\Gamma_s = \pi\tau^2 \nu_n / d_s$ and the normal metal $\Gamma_n = \pi\tau^2 \nu_s / d_n$ and $d_s = V_s/S$ and $d_n = V_n/S$ are the thicknesses of the superconducting and normal layers, respectively.

III. DYNAMICAL EQUATIONS FOR THE ORDER PARAMETER

In order to study the near-equilibrium dynamics of the system we expand the order parameter near Δ_0 while assuming its phase is zero in equilibrium without loss of generality:

$$\Delta(t) = \Delta_0 + \delta\Delta(t) + i\Delta_0 \delta\theta(t). \tag{22}$$

Here $\delta\Delta$ and $\delta\theta$ are the perturbations of the magnitude and the phase of Δ, respectively. One can introduce the corresponding perturbations to the Green's functions and the self-energies:

$$\begin{aligned} \check{G}_k^s &= \check{G}_{0k}^s + \delta\check{G}_k^s, \ \check{G}_k^n = \check{G}_{0l}^n + \delta\check{G}_l^n, \\ \check{\Sigma}^{s/n} &= \check{\Sigma}_0^{s/n} + \delta\check{\Sigma}^{s/n}, \end{aligned} \tag{23}$$

where $\check{G}_{0k}^s$, $\check{G}_{0l}^n$, and $\check{\Sigma}_0^{s/n}$ are the equilibrium Green's functions and self-energies of the superconductor and the normal metal accounting for tunneling. The Dyson equations should also be linearized with respect to $\delta\Delta$ and $\delta\theta$, so the closed set of equations for the linear perturbations of the Green's functions and the self-energies reads

$$\begin{aligned} &i\frac{\partial}{\partial t}\delta\check{G}_k^s - H_{0k}^s \delta G_k^s - \Sigma^s * \delta\check{G}_k^s - \delta\Sigma^s * \check{G}_{0k}^s = \delta H^s G_{0k}^s, \\ &i\frac{\partial}{\partial t}\delta\check{G}_l^n - H_l^n \delta G_l^n - \Sigma^n * \delta\check{G}_l^n - \delta\Sigma^n * \check{G}_{0l}^n = 0, \\ &\delta\check{\Sigma}^s = \frac{\Gamma_s}{\pi} \int \check{\tau}_3 \delta\check{G}_l^n \check{\tau}_3 \, d\xi_l^n, \\ &\delta\check{\Sigma}^n = \frac{\Gamma_n}{\pi} \int \check{\tau}_3 \delta\check{G}_k^s \check{\tau}_3 \, d\xi_k^s. \end{aligned} \tag{24}$$

The perturbation to the single-mode Hamiltonian of the superconductor is $\delta\check{H}^s = \delta\Delta\check{\tau}_1 - i\Delta_0\delta\theta\check{\tau}_2$, where $\check{\tau}_j$ are the 4×4 Pauli matrices in Keldysh-Nambu space:

$$\check{\tau}_j = \begin{pmatrix} \check{\tau}_j & 0 \\ 0 & \check{\tau}_j \end{pmatrix} \tag{25}$$

One can easily solve the equations for δG in the Fourier form:

$$\begin{aligned} \delta\check{G}_k^s(\omega,\omega') &= \check{G}_{0k}^s(\omega)[\delta\check{H}^s(\omega-\omega') + \delta\check{\Sigma}^s(\omega,\omega')]\check{G}_{0k}^s(\omega'), \\ \delta\check{G}_l^n(\omega,\omega') &= \check{G}_{0l}^n(\omega)\delta\check{\Sigma}^n(\omega,\omega')\check{G}_{0l}^n(\omega'), \end{aligned} \tag{26}$$

where the Fourier transform of the Green's functions is defined as follows:

$$\begin{aligned} \delta\check{G}(t,t') &= \frac{1}{(2\pi)^2} \int \delta\check{G}(\omega,\omega') e^{-i\omega t + i\omega' t'} \, d\omega \, d\omega', \\ \check{G}_0(t-t') &= \frac{1}{2\pi} \int \check{G}_0(\omega) e^{-i\omega(t-t')} \, d\omega. \end{aligned} \tag{27}$$

We introduce the quasiclassic Green's function $\delta\check{g}^s = \int \delta\check{G}_k^s \, d\xi_k^s$ and write an algebraic equation for it:

$$\begin{aligned} \delta\check{g}(\omega,\omega') = &\int \check{G}_{0k}^s(\omega)\delta\check{H}_k(\omega-\omega')\check{G}_{0k}^s(\omega') \, d\xi_k^s \\ &+ \frac{\Gamma_n\Gamma_s}{\pi^2} \int \check{G}_{0k}^s(\omega)\check{\tau}_3\check{G}_{0l}^n(\omega)\check{\tau}_3\delta\check{g}(\omega,\omega') \\ &\times \check{\tau}_3\check{G}_{0l}^n(\omega')\check{\tau}_3\check{G}_{0k}^s(\omega') \, d\xi_k^s \, d\xi_l^n. \end{aligned} \tag{28}$$

The above equation can be considered a system of 12 linear equations for the 12 components of the matrix Green's function $\check{g}(\omega,\omega')$ (retarded, advanced, and Keldysh, each of which is a 2×2 matrix). Each integral can be evaluated

analytically because the equilibrium Green's functions are rational functions of the normal energies ξ_k^s and ξ_l^n. The solution can be written in the following form:

$$\delta\check{g}(\omega,\omega') = \check{A}_\Delta(\omega,\omega')\delta\Delta(\omega-\omega') + \Delta_0\check{A}_\theta(\omega,\omega')\delta\theta(\omega-\omega'). \tag{29}$$

One should use the self-consistency equation (10)

$$\delta\Delta(\omega) = \frac{i\lambda\nu_s}{8\pi}\int \mathrm{Tr}\,\check{\tau}_1\delta\check{g}^{(K)}(\omega'+\omega,\omega')\,d\omega',$$
$$\delta\theta(\omega) = \frac{i\lambda\nu_s}{8\pi\Delta_0}\int \mathrm{Tr}\,\check{\tau}_2\delta\check{g}^{(K)}(\omega'+\omega,\omega')\,d\omega' \tag{30}$$

and write down the equations for the frequencies of the eigenmodes of $\delta\Delta$ and $\delta\theta$:

$$\delta\Delta(\omega) = K_\Delta(\omega)\delta\Delta(\omega) + K'(\omega)\Delta_0\delta\theta(\omega),$$
$$\delta\theta(\omega) = K''(\omega)\frac{\delta\Delta(\omega)}{\Delta_0} + K_\theta(\omega)\delta\theta(\omega), \tag{31}$$

where the expression for the kernels is given as follows:

$$K_\Delta(\omega) = \frac{i\lambda\nu_s}{8\pi}\int \mathrm{Tr}\,\check{\tau}_1\check{A}_\Delta^{(K)}(\omega'+\omega,\omega')\,d\omega',$$
$$K'(\omega) = \frac{i\lambda\nu_s}{8\pi}\int \mathrm{Tr}\,\check{\tau}_1\check{A}_\theta^{(K)}(\omega'+\omega,\omega')\,d\omega',$$
$$K''(\omega) = \frac{i\lambda\nu_s}{8\pi}\int \mathrm{Tr}\,\check{\tau}_2\check{A}_\Delta^{(K)}(\omega'+\omega,\omega')\,d\omega',$$
$$K_\theta(\omega) = \frac{i\lambda\nu_s}{8\pi}\int \mathrm{Tr}\,\check{\tau}_2\check{A}_\theta^{(K)}(\omega'+\omega,\omega')\,d\omega'. \tag{32}$$

The off-diagonal kernels K' and K'' are equal exactly to zero in the systems which have electron-hole symmetry and can be neglected if the Fermi level in both the superconductor and the normal metal is far from the Van Hove singularities in the density of states [40]. The singular points of $[1-K_\Delta(\omega)]^{-1}$ and $[1-K_\theta(\omega)]^{-1}$ correspond to the frequencies of the Higgs and Anderson-Bogoliubov modes of the superconductor. The perturbations of the magnitude and the phase of the order parameter are completely independent, so hereafter, we focus only on the study of the Higgs modes.

The linear response of the superconducting order parameter to an external force $f(\omega)$ takes the following form:

$$\delta\Delta(t) = \frac{1}{2\pi}\int \frac{f(\omega)e^{-i\omega t}\,d\omega}{1-K_\Delta(\omega)}. \tag{33}$$

Previous studies [32–34,41] show that this force can originate, e.g., from the pulses of the external electromagnetic field.

The results of numerical evaluation of Eqs. (28), (29), and (32) are shown in Fig. 3, where the typical frequency dependencies of the real and imaginary parts of $[1-K_\Delta(\omega)]^{-1}$ are shown for some particular values of the tunneling rates in the zero-temperature limit $T=0$. The spectrum of the Higgs modes appears to be consistent with the picture shown in Fig. 1. The broadened features at the frequencies $\omega\approx\pm2\Delta_0$ and $\omega\approx\pm(\Delta_0+\Delta_i)$ are seen clearly, while the singularity at $\omega=\pm2\Delta_i$ can be seen only in the zoomed-in inset. The latter singularity corresponds to the low-frequency Higgs mode [Fig. 1(c)]. This mode has no exponential damping as Δ_i is a hard gap of the whole system (the singular point

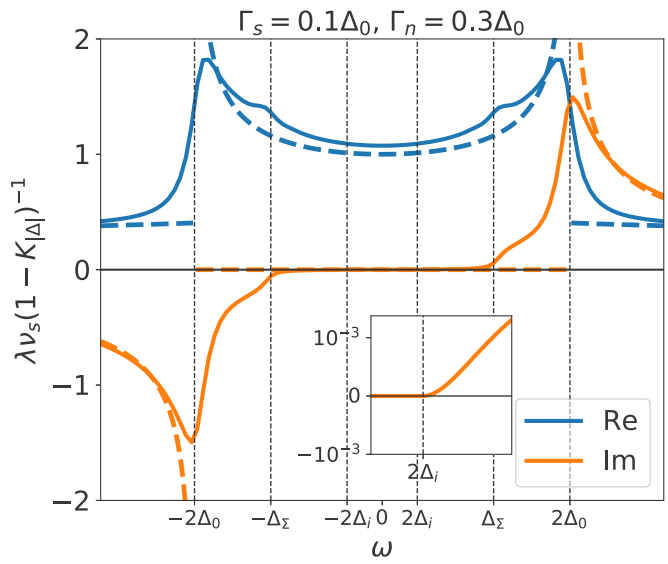

FIG. 3. The real and imaginary parts of $[1-K_\Delta(\omega)]^{-1}$ in the case of the finite tunneling rates Γ_s and Γ_n. The inset shows the singularity at frequency $2\Delta_i$ which cannot be observed in the regular scale. For the given parameters $\Gamma_s=0.1\Delta_0$ and $\Gamma_n=0.3\Delta_0$ the induced gap Δ_i is approximately equal to $0.2\Delta_0$. Here $\Delta_\Sigma=\Delta_0+\Delta_i$. The dashed line shows $[1-K_\Delta(\omega)]^{-1}$ for the isolated superconductor $\Gamma_s=\Gamma_n=0$.

of the kernel is exactly at the real axis). This means that this low-frequency mode gives the major contribution to the oscillations of the order parameter in the long-time limit, $t\gg\Gamma_s^{-1},\Gamma_n^{-1}$; however, the amplitude of this mode is a few orders of magnitude lower than the amplitude of the usual Higgs mode due to the low transparency of the insulating barrier.

IV. ZERO-INDUCED-GAP LIMIT $\Delta_i = 0$

In this section we consider the analytically tractable case of the zero-temperature limit and $\Gamma_n=0$, which corresponds to the bulk normal metal $V_n\to\infty$ with suppressed induced superconducting ordering and vanishing induced gap $\Delta_i=0$. In the Sec. IV A and IV B detailed calculations of the kernel (32) and the linear response for the order parameter (33) are given, with the main results summed up in Eqs. (40) and (44).

A. Evaluation of the kernel K_Δ

In the above-mentioned limit the kernel K_Δ can be evaluated analytically. In this case the self-energies of the superconductor are determined by the equilibrium Green's functions of the normal metal, and in the zero-temperature limit we have

$$\check{\Sigma}^{s(R/A)}(\omega) = \pm i\Gamma_s,\ \check{\Sigma}^{s(K)}(\omega) = -2i\Gamma_s\mathrm{sgn}\omega \tag{34}$$

$$\check{G}_{0k}^{s(R/A)} = \left(\omega\pm i\Gamma_s - \check{H}_{0k}^s\right)^{-1}, \tag{35}$$

$$\check{G}_{0k}^{s(K)} = \left[\check{G}_{0k}^{s(R)} - \check{G}_{0k}^{s(A)}\right]\mathrm{sgn}\omega. \tag{36}$$

The self-energies are constant $\delta\Sigma^s=0$, so the solution of Eqs. (24) takes the following form:

$$\delta\check{G}_k^s(\omega,\omega') = \check{G}_{0k}^s(\omega)\delta\check{H}^s(\omega-\omega')\check{G}_{0k}^s(\omega'). \tag{37}$$

Using the self-consistency equation (10), one can obtain an expression for the kernel of the Higgs mode:

$$K_\Delta(\omega) = \frac{i\lambda\nu_s}{8\pi}\iint \mathrm{Tr}\left[\check{\tau}_1\check{G}^{s(R)}_{0k}(\omega+\omega')\check{\tau}_1\check{G}^{s(K)}_{0k}(\omega') + \check{\tau}_1\check{G}^{s(K)}_{0k}(\omega'+\omega)\check{\tau}_1\check{G}^{s(A)}_{0k}(\omega')\right] d\omega'\, d\xi^s_k. \quad (38)$$

This integral diverges logarithmically; however, it can be regularized using the equilibrium self-consistency equation for Δ_0:

$$1 = \frac{i\lambda\nu_s}{8\pi\Delta_0}\int \mathrm{Tr}\,\check{\tau}_1 G^{s(K)}_{0k}(\omega)\, d\omega\, d\xi^s_k. \quad (39)$$

Finally, after long but straightforward calculations one can obtain the following expression for the kernel of the Higgs mode:

$$\frac{1-K_\Delta(\omega)}{\lambda\nu_s} = i\frac{\sqrt{4\Delta_0^2-\omega^2}}{2\omega}\ln\left[\frac{2\Delta_0^2+i\Gamma_s\omega+\sqrt{\Gamma_s^2+\Delta_0^2}\sqrt{4\Delta_0^2-\omega^2}}{2\Delta_0^2-\omega(\omega+i\Gamma_s)+\sqrt{4\Delta_0^2-\omega^2}\sqrt{\Delta_0^2-(\omega+i\Gamma_s)^2}}\frac{\omega+i\sqrt{4\Delta_0^2-\omega^2}}{-\omega+i\sqrt{4\Delta_0^2-\omega^2}}\right] + i\frac{\sqrt{4\Delta_0^2-(\omega+2i\Gamma_s)^2}}{2\omega+4i\Gamma_s}\ln\left[\frac{2\Delta_0^2-(\omega+2i\Gamma_s)(\omega+i\Gamma_s)+\sqrt{4\Delta_0^2-(\omega+2i\Gamma_s)^2}\sqrt{\Delta_0^2-(\omega+i\Gamma_s)^2}}{2\Delta_0^2-i\Gamma_s(\omega+2i\Gamma_s)+\sqrt{4\Delta_0^2-(\omega+2i\Gamma_s)^2}\sqrt{\Gamma_s^2+\Delta_0^2}}\right]. \quad (40)$$

In the isolated superconductor, $\Gamma_s = 0$, the kernel as a function of the complex frequency ω has two branch points at $\omega = \pm 2\Delta_0$ which give the usual polynomially damped Higgs mode in the superconductor. In the presence of tunneling, $\Gamma_s > 0$, these branch points shift to the points $\omega = \pm 2\Delta_0 - 2i\Gamma_s$ corresponding to exponential damping of this mode. Moreover, two additional branch points at $\omega = \pm\Delta_0 - i\Gamma_s$ appear, triggering a new Higgs mode, which has already revealed itself in Fig. 3. The absence of the low-frequency mode at $2\Delta_i$ is rather expected for the considered case $\Gamma_n = 0$ because the electrons of the normal metal are not affected by the proximity with the superconductor and thus cannot form a Cooper pair as in Fig. 1(c). As a result they do not contribute to the order parameter oscillations.

B. Evaluation of the order parameter linear response

The integral (33) can be evaluated if we close the integration contour as shown in Fig. 4:

$$\frac{1}{2\pi}\oint_{\mathcal{C}}\frac{f(\omega)e^{-i\omega t}\,d\omega}{1-K_\Delta(\omega)} = -i\sum_j \frac{e^{-i\omega_j t}\,\mathrm{res}_{\omega_j} f(\omega)}{1-K_\Delta(\omega_j)}, \quad (41)$$

where $\mathcal{C}$ is the integration contour, ω_j are the poles of the external force $f(\omega)$ within the contour $\mathcal{C}$, and $\mathrm{res}_{\omega_j} f(\omega)$ is the residue of $f(\omega)$ at the pole ω_j. Thus, the integral in Eq. (33) can be expressed as a sum of the integrals along the branch cuts and the terms with the residues of the external force:

$$\delta\Delta(t) = -i\sum_j \frac{e^{-i\omega_j t}\,\mathrm{res}_{\omega_j} f(\omega)}{1-K_\Delta(\omega_j)} - \frac{1}{2\pi}\left\{\int_{\Delta_0-i\Gamma_s}^{+\infty-i\Gamma_s}\left[\frac{f(\omega)e^{-i\omega t}}{1-K_\Delta(\omega-i0)}-\frac{f(\omega)e^{-i\omega t}}{1-K_\Delta(\omega+i0)}\right]d\omega + \int_{2\Delta_0-2i\Gamma_s}^{+\infty-2i\Gamma_s}\left[\frac{f(\omega)e^{-i\omega t}}{1-K_\Delta(\omega-i0)}-\frac{f(\omega)e^{-i\omega t}}{1-K_\Delta(\omega+i0)}\right]d\omega + \int_{-\infty-2i\Gamma_s}^{-2\Delta_0-2i\Gamma_s}\left[\frac{f(\omega)e^{-i\omega t}}{1-K_\Delta(\omega-i0)}-\frac{f(\omega)e^{-i\omega t}}{1-K_\Delta(\omega+i0)}\right]d\omega + \int_{-\infty-i\Gamma_s}^{-\Delta_0-i\Gamma_s}\left[\frac{f(\omega)e^{-i\omega t}}{1-K_\Delta(\omega-i0)}-\frac{f(\omega)e^{-i\omega t}}{1-K_\Delta(\omega+i0)}\right]d\omega\right\}. \quad (42)$$

The integrals along the branch cuts can be evaluated approximately assuming $f(\omega)$ is regular near the branch points of $K_\Delta(\omega)$. Also we suppose that the main contribution to these integrals comes from the vicinity of the singularities. The expansion of the kernel $K_\Delta(\omega)$ near its branch points at $\omega = \pm 2\Delta_0 - 2i\Gamma_s$ and $\omega = \pm\Delta_0 - i\Gamma_s$ in the limit $\Gamma_s \ll \Delta_0$ reads as follows:

$$\begin{aligned}
\omega &= \Delta_0 - i\Gamma_s + \Omega: && \frac{1-K_\Delta}{\lambda\nu_s} \approx \frac{\pi}{2\sqrt{3}} + \frac{2\Gamma_s\sqrt{-2\Omega}}{\Delta_0^{3/2}},\\
\omega &= -\Delta_0 - i\Gamma_s - \Omega: && \frac{1-K_\Delta}{\lambda\nu_s} \approx \frac{\pi}{2\sqrt{3}} - \frac{2\Gamma_s\sqrt{-2\Omega}}{\Delta_0^{3/2}},\\
\omega &= 2\Delta_0 - 2i\Gamma_s + \Omega: && \frac{1-K_\Delta}{\lambda\nu_s} \approx \pi(1+i)\sqrt{\frac{\Gamma_s}{\Delta_0}} + \frac{\pi}{2}\sqrt{-\frac{\Omega}{\Delta_0}},\\
\omega &= -2\Delta_0 - 2i\Gamma_s - \Omega: && \frac{1-K_\Delta}{\lambda\nu_s} \approx \pi(1-i)\sqrt{\frac{\Gamma_s}{\Delta_0}} - \frac{\pi}{2}\sqrt{-\frac{\Omega}{\Delta_0}}.
\end{aligned} \quad (43)$$

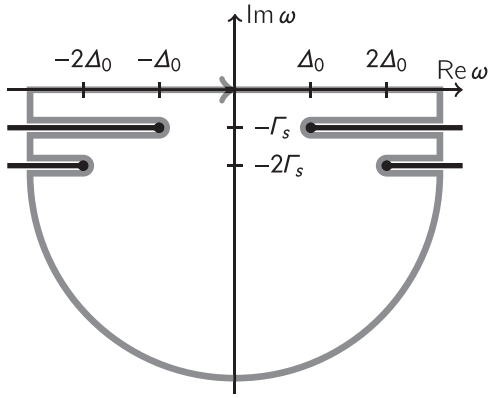

FIG. 4. Area of analyticity of the kernel K_Δ. The four black dots are the branch points $\omega = \pm\Delta_0 - i\Gamma_s$ and $\omega = \pm 2\Delta_0 - 2i\Gamma_s$; the thick black lines are the branch cuts. The thick gray line shows the integration contour in Eq. (41).

Using these expansions, one can finally obtain an asymptotic expression for the near-equilibrium oscillations of the superconducting gap in the intermediate-time limit $\Delta_0^{-1} \ll t \ll \Gamma_s^{-1}$:

$$\delta\Delta(t) \approx -i\sum_j \frac{e^{-i\omega_j t}\,\mathrm{res}_{\omega_j} f(\omega)}{1 - K_\Delta(\omega_j)} + \frac{1}{2\pi\lambda\nu_s}\left\{\frac{12\sqrt{2}\Gamma_s e^{-\Gamma_s t}\left[f(\Delta_0)e^{-i\Delta_0 t - i\frac{\pi}{4}} + \text{c.c.}\right]}{(\pi\Delta_0 t)^{3/2}} + \frac{2\sqrt{\Delta_0}e^{-2\Gamma_s t}\left[f(2\Delta_0)e^{-2i\Delta_0 t + i\frac{\pi}{4}} + \text{c.c.}\right]}{(\pi t)^{1/2}}\right\}. \quad (44)$$

The first term in (44) describes the forced oscillations of the order parameter which occur at the frequencies corresponding to the poles of the Fourier spectrum of the external force $f(\omega)$. The finite tunneling rate Γ_s leads to the exponential damping of the oscillations of the order parameter and the appearance of a new Higgs mode at the frequency Δ_0, with the magnitude suppressed by the factor Γ_s/Δ_0. This mode corresponds to the middle-frequency mode $\Delta_0 + \Delta_i$ shown in Fig. 1(b) in the limit $\Delta_i = 0$. Let's emphasize once again that all of the above analysis was related to the case of the small tunneling rates $\Gamma_s \ll \Delta_0$. In the opposite limit $\Gamma_s \gg \Delta_0$ we get the gapless superconductivity with a pure imaginary frequency of the Higgs mode: $\omega = -i\Delta_0^2/\Gamma_s$. The relaxation of the order parameter in this limit is described by the decaying exponent $\delta\Delta(t) \propto \exp(-\Delta_0^2 t/\Gamma_s)$.

V. DISCUSSION

The Higgs modes of the SIN system can be studied using a pump-probe experiment similar to the one developed in Ref. [32]. The measured $\delta\Delta(t)$ can be analyzed using the Fourier transform. The Fourier spectrum is expected to have two peaks at $\omega \approx 2\Delta_0$ and $\omega \approx \Delta_0 + \Delta_i$, corresponding to the above Higgs modes of the SIN system. In the limit of low transparency $D \ll 1$ the mode with the frequency $2\Delta_i$ has too low magnitude, so its experimental observation can be hampered; however, it may be visible at intermediate transparencies $D \sim 1$, $\Delta_i \lesssim \Delta_0$. Another way to detect the Higgs modes is the experimental study of the frequency dependence of the third-harmonic generation [33,34]. The electromagnetic wave with frequency Ω excites the Higgs mode with frequency 2Ω. The magnitude of the generated nonlinear signal with frequency 3Ω should depend on the magnitude of the oscillations of the order parameter, and therefore, one can expect the appearance of the broadened resonances in the third-harmonic response if the frequency 2Ω is close to the frequency of any of the Higgs modes. However, the effect of generation of nonequilibrium quasiparticles by the electromagnetic radiation with frequency $\Omega > 2\Delta_i$ may complicate the observation of the resonant effect in the third-harmonic generation. The overheating can be significantly reduced at intermediate transparencies $D \sim 1$ when the induced gap is high enough $3\Delta_i > \Delta_0$. This improves the observability of the resonance at $2\Omega = \Delta_0 + \Delta_i$ predicted above. Also in the case of a finite temperature the inelastic processes such as electron-phonon scattering [42] should lead to the damping of the Higgs modes and may complicate their observability. The influence of the inelastic processes is expected to be stronger in the normal metal than in the superconductor due to the lower induced gap $\Delta_i < \Delta_0$ and higher density of the equilibrium quasiparticles. Thus, the low-frequency modes should be affected more strongly than the usual $2\Delta_0$ mode. However, the inelastic processes may be suppressed if the temperature is well below the induced gap $T \ll \Delta_i$ when there are no equilibrium quasiparticles in the system.

The dynamical effects considered here are relevant for various systems with proximity-induced superconductivity in both the usual metals [43] and topologically nontrivial materials [44–47]. Note that the parameters $\Gamma_s \sim 0.1\Delta_0$, $\Gamma_n \sim 0.3\Delta_0$ used in Fig. 3 are rather typical for all above-mentioned experiments with transparent SN junctions. The corresponding frequencies lie in the same sub-THz range as in the experimental papers [32,33] probing Higgs modes in purely superconducting samples.

VI. CONCLUSION

To sum up, the effect of the quasiparticle spectrum of the superconducting system on the low-temperature dynamics of the order parameter has been studied using an example of a hybrid superconductor-insulator-normal metal system. Two additional Higgs modes in such system have been discovered. The frequencies of these modes are formed by sums of the two quasiparticle energies, which are in good agreement with the qualitative interpretation of the Higgs modes as coherent processes of splitting and recovery of the Cooper pairs (Fig. 1). The proposals of experimental observation of these Higgs modes in a hybrid SIN system have been developed on the basis of the existing THz techniques used to study the Higgs modes in pure superconductors.

ACKNOWLEDGMENTS

We thank S. V. Sharov for stimulating discussions. This work was supported, in part, by the Russian Foundation for Basic Research under Grants No. 17-52-12044 and

No. 18-02-00390, the Foundation for the Advancement to Theoretical Physics and Mathematics "BASIS" Grant No. 17-11-109, and the German-Russian Interdisciplinary Science Center (G-RISC) funded by the German Federal Foreign Office via the German Academic Exchange Service (DAAD). For the numerical calculations, the work was supported by the Russian Science Foundation (Grant No. 17-12-01383). I.M.K. acknowledges the support of the German Research Foundation (DFG), Grant No. KH 425/1-1. V.L.V. and A.S.M. appreciate the warm hospitality the Max-Planck Institute for the Physics of Complex Systems, Dresden, Germany, extended to them during their visits when this work was done.

[1] Y. Oreg, G. Refael, and F. v. Oppen, Helical Liquids and Majorana Bound States in Quantum Wires, Phys. Rev. Lett. **105**, 177002 (2010).

[2] X.-L. Qi and Sh.-Ch. Zhang, Topological insulators and superconductors, Rev. Mod. Phys. **83**, 1057 (2011).

[3] M. Sato and Y. Ando, Topological superconductors: A review, Rep. Prog. Phys. **80**, 076501 (2017).

[4] H. B. Heersche, P. Jarillo-Herrero, J. B. Oostinga, L. M. K. Vandersypen, and A. F. Morpurgo, Induced superconductivity in graphene, Solid State Commun. **143**, 72 (2007).

[5] T. Sato, T. Moriki, S. Tanaka, A. Kanda, H. Goto, H. Miyazaki, S. Odaka, Y. Ootuka, K. Tsukagoshi, and Y. Aoyagi, Gate-controlled superconducting proximity effect in ultrathin graphite films, Phys. E (Amsterdam) **40**, 1495 (2008).

[6] N. B. Kopnin, I. M. Khaymovich, and A. S. Mel'nikov, Predicted Multiple Cores of a Magnetic Vortex Threading a Two-Dimensional Metal Proximity Coupled to a Superconductor, Phys. Rev. Lett. **110**, 027003 (2013).

[7] N. B. Kopnin, I. M. Khaymovich, and A. S. Mel'nikov, Vortex matter in low-dimensional systems with proximity-induced superconductivity, J. Exp. Theor. Phys. **117**, 418 (2013).

[8] G.-H. Lee and H.-J. Lee, Proximity coupling in superconductor-graphene heterostructures, Rep. Prog. Phys. **81**, 056502 (2018).

[9] R. M. Lutchyn, E. P. A. M. Bakkers, L. P. Kouwenhoven, P. Krogstrup, C. M. Marcus, and Y. Oreg, Majorana zero modes in superconductor–semiconductor heterostructures, Nat. Rev. Mater. **3**, 52 (2018).

[10] D. Aasen, M. Hell, R. V. Mishmash, A. Higginbotham, J. Danon, M. Leijnse, T. S. Jespersen, J. A. Folk, C. M. Marcus, K. Flensberg, and J. Alicea, Milestones Toward Majorana-Based Quantum Computing, Phys. Rev. X **6**, 031016 (2016).

[11] J. Alicea, New directions in the pursuit of Majorana fermions in solid state systems, Rep. Prog. Phys. **75**, 076501 (2012).

[12] I. M. Khaymovich, J. P. Pekola, and A. S. Melnikov, Nonlocality and dynamic response of Majorana states in fermionic superfluids, New J. Phys. **19**, 123026 (2017).

[13] G. W. Semenoff and P. Sodano, Stretched quantum states emerging from a Majorana medium, J. Phys. B **40**, 1479 (2007).

[14] S. Tewari, Ch. Zhang, S. DasSarma, C. Nayak, and D.-H. Lee, Testable Signatures of Quantum Nonlocality in a Two-Dimensional Chiral p-Wave Superconductor, Phys. Rev. Lett. **100**, 027001 (2008).

[15] L. Fu, Electron Teleportation via Majorana Bound States in a Mesoscopic Superconductor, Phys. Rev. Lett. **104**, 056402 (2010).

[16] C. J. Bolech and E. Demler, Observing Majorana Bound States in p-Wave Superconductors using Noise Measurements in Tunneling Experiments, Phys. Rev. Lett. **98**, 237002 (2007).

[17] J. Nilsson, A. R. Akhmerov, and C. W. J. Beenakker, Splitting of a Cooper Pair by a Pair of Majorana Bound States, Phys. Rev. Lett. **101**, 120403 (2008).

[18] A. V. Semenov, I. A. Devyatov, P. J. de Visser, and T. M. Klapwijk, Coherent Excited States in Superconductors Due to a Microwave Field, Phys. Rev. Lett. **117**, 047002 (2016).

[19] I. A. Devyatov and A. V. Semenov, Relaxation of coherent excited states of a superconductor to a superconducting reservoir, JETP Lett. **109**, 256 (2019).

[20] N. Bittner, D. Einzel, L. Klam, and D. Manske, Leggett Modes and the Anderson-Higgs Mechanism in Superconductors without Inversion Symmetry, Phys. Rev. Lett. **115**, 227002 (2015).

[21] H. Krull, N. Bittner, G. S. Uhrig, D. Manske, and A. P. Schnyder, Coupling of Higgs and Leggett modes in nonequilibrium superconductors, Nat. Commun. **7**, 11921 (2016).

[22] B. Fauseweh, L. Schwarz, N. Tsuji, N. Cheng, N. Bittner, H. Krull, M. Berciu, G. S. Uhrig, A. P. Schnyder, S. Kaiser, and D. Manske, Higgs spectroscopy of superconductors in nonequilibrium, arXiv:1712.07989.

[23] A. F. Volkov and S. M. Kogan, Collisionless relaxation of energy-gap in superconductors, Zh. Eksp. Teor. Fiz. **65**, 2038 (1974) [Sov. Phys. JETP **38**, 1018 (1974)].

[24] E. A. Yuzbashyan, V. B. Kuznetsov, and B. L. Altshuler, Integrable dynamics of coupled Fermi-Bose condensates, Phys. Rev. B **72**, 144524 (2005).

[25] E. A. Yuzbashyan, O. Tsyplyatyev, and B. L. Altshuler, Relaxation and Persistent Oscillations of the Order Parameter in Fermionic Condensates, Phys. Rev. Lett. **96**, 097005 (2006).

[26] E. A. Yuzbashyan and M. Dzero, Dynamical Vanishing of the Order Parameter in a Fermionic Condensate, Phys. Rev. Lett. **96**, 230404 (2006).

[27] E. A. Yuzbashyan, O. Tsyplyatyev, and B. L. Altshuler, Erratum: Relaxation and Persistent Oscillations of the Order Parameter in Fermionic Condensates [Phys. Rev. Lett. **96**, 097005 (2006)], Phys. Rev. Lett. **96**, 179905(E) (2006).

[28] P. W. Higgs, Broken Symmetries and the Masses of Gauge Bosons, Phys. Rev. Lett. **13**, 508 (1964).

[29] R. A. Barankov, L. S. Levitov, and B. Z. Spivak, Collective Rabi Oscillations and Solitons in a Time-Dependent BCS Pairing Problem, Phys. Rev. Lett. **93**, 160401 (2004).

[30] R. Sooryakumar and M. V. Klein, Raman Scattering by Superconducting-Gap Excitations and Their Coupling to Charge-Density Waves, Phys. Rev. Lett. **45**, 660 (1980).

[31] M.-A. Méasson, Y. Gallais, M. Cazayous, B. Clair, P. Rodière, L. Cario, and A. Sacuto, Amplitude Higgs mode in the $2H$-$NbSe_2$ superconductor, Phys. Rev. B **89**, 060503(R) (2014).

[32] R. Matsunaga, Y. I. Hamada, K. Makise, Y. Uzawa, H. Terai, Zh. Wang, and R. Shimano, Higgs Amplitude Mode in the BCS Superconductors $Nb_{1-x}Ti_xN$ Induced by Terahertz Pulse Excitation, Phys. Rev. Lett. **111**, 057002 (2013).

[33] R. Matsunaga, N. Tsuji, H. Fujita, A. Sugioka, K. Makise, Y. Uzawa, H. Terai, Zh. Wang, H. Aoki, and R. Shimano, Light-induced collective pseudospin precession resonating with Higgs mode in a superconductor, Science **345**, 1145 (2014).

[34] M. Silaev, Nonlinear electromagnetic response and Higgs-mode excitation in BCS superconductors with impurities, Phys. Rev. B **99**, 224511 (2019).

[35] A. Moor, A. F. Volkov, and K. B. Efetov, Amplitude Higgs Mode and Admittance in Superconductors with a Moving Condensate, Phys. Rev. Lett. **118**, 047001 (2017).

[36] W. L. McMillan, Tunneling model of the superconducting proximity effect, Phys. Rev. **175**, 537 (1968).

[37] The corresponding equilibrium models with a clean interface as well as clean and dirty limits of the superconducting lead were considered in Refs. [6,7,39,48,49].

[38] A. F. Volkov, P. H. C. Magnée, B. J. Van Wees, and T. M. Klapwijk, Proximity and Josephson effects in superconductor-two-dimensional electron gas planar junctions, Phys. C (Amsterdam, Neth.) **242**, 261 (1995).

[39] N. B. Kopnin and A. S. Melnikov, Proximity-induced superconductivity in two-dimensional electronic systems, Phys. Rev. B **84**, 064524 (2011).

[40] For example, in proximized semiconducting nanowires [1,9,10] the phase transition from the trivial to topological phase occurs at such a Van Hove singularity, which strongly affects the superconducting properties of the system [50].

[41] N. Tsuji and H. Aoki, Theory of Anderson pseudospin resonance with Higgs mode in superconductors, Phys. Rev. B **92**, 064508 (2015).

[42] S. B. Kaplan, C. C. Chi, D. N. Langenberg, J. J. Chang, S. Jafarey, and D. J. Scalapino, Quasiparticle and phonon lifetimes in superconductors, Phys. Rev. B **14**, 4854 (1976).

[43] V. S. Stolyarov, T. Cren, C. Brun, I. A. Golovchanskiy, O. V. Skryabina, D. I. Kasatonov, M. M. Khapaev, M. Yu. Kupriyanov, A. A. Golubov, and D. Roditchev, Expansion of a superconducting vortex core into a diffusive metal, Nat. Commun. **9**, 2277 (2018).

[44] W. Chang, S. M. Albrecht, T. S. Jespersen, F. Kuemmeth, P. Krogstrup, J Nygård, and C. M. Marcus, Hard gap in epitaxial semiconductor–superconductor nanowires, Nat. Nanotechnol. **10**, 232 (2015).

[45] E. Bocquillon, R. S. Deacon, J. Wiedenmann, P. Leubner, T. M. Klapwijk, C. Brüne, K. Ishibashi, H. Buhmann, and L. W. Molenkamp, Gapless Andreev bound states in the quantum spin Hall insulator HgTe, Nat. Nanotechnol. **12**, 137 (2017).

[46] J. Wiedenmann, E. Bocquillon, R. S. Deacon, S. Hartinger, O. Herrmann, T. M. Klapwijk, L. Maier, C. Ames, C. Brüne, C. Gould *et al.*, 4π-periodic Josephson supercurrent in HgTe-based topological Josephson junctions, Nat. Commun. **7**, 10303 (2016).

[47] R. S. Deacon, J. Wiedemann, E. Bocquillon, T. M. Klapwijk, C. Aames, C. Brüne, S. Tarucha, K. Ishibashi, H. Buhmann, and L. W. Molenkamp, Searching for Majorana modes in HgTe topological insulator Josephson junctions, AAPPS Bull. **26**, 20 (2016).

[48] I. A. Devyatov, M. Yu. Romashka, and A. V. Burmistrova, Current and heat transfer through the interface between a two-band superconductor and a normal metal, JETP Lett. **91**, 297 (2010).

[49] A. V. Burmistrova, T. Yu. Karminskaya, and I. A. Devyatov, Electron transport across the interface of a normal metal and a two-band superconductor with interband pairing, JETP Lett. **93**, 133 (2011).

[50] A. A. Kopasov, I. M. Khaymovich, and A. S. Mel'nikov, Inverse proximity effect in semiconductor Majorana nanowires, Beilstein J. Nanotechnol. **9**, 1184 (2018).